RSC Advances

PAPER

View Article Online
View Journal | View Issue

Cite this: *RSC Adv.*, 2024, **14**, 13734

In vitro encapsulation and expansion of T and CAR-T cells using 3D synthetic thermo-responsive matrices†

Gaby D. Lizana-Vasquez,[a] Janet Mendez-Vega,[a] Dan Cappabianca,[b] Krishanu Saha[b] and Madeline Torres-Lugo*[a]

Suspension cell culture and rigid commercial substrates are the most common methods to clinically manufacture therapeutic CAR-T cells *ex vivo*. However, suspension culture and nano/micro-scale commercial substrates poorly mimic the microenvironment where T cells naturally develop, leading to profound impacts on cell proliferation and phenotype. To overcome this major challenge, macro-scale substrates can be used to emulate that environment with higher precision. This work employed a biocompatible thermo-responsive material with tailored mechanical properties as a potential synthetic macro-scale scaffold to support T cell encapsulation and culture. Cell viability, expansion, and phenotype changes were assessed to study the effect of two thermo-responsive hydrogel materials with stiffnesses of 0.5 and 17 kPa. Encapsulated Pan-T and CAR-T cells were able to grow and physically behave similar to the suspension control. Furthermore, matrix stiffness influenced T cell behavior. In the softer polymer, T cells had higher activation, differentiation, and maturation after encapsulation obtaining significant cell numbers. Even when terpolymer encapsulation affected the CAR-T cell viability and expansion, CAR T cells expressed favorable phenotypical profiles, which was supported with cytokines and lactate production. These results confirmed the biocompatibility of the thermo-responsive hydrogels and their feasibility as a promising 3D macro-scale scaffold for *in vitro* T cell expansion that could potentially be used for cell manufacturing process.

Received 14th March 2024
Accepted 17th April 2024

DOI: 10.1039/d4ra01968g

rsc.li/rsc-advances

1. Introduction

Adoptive T cell therapy is a successful treatment against hematological malignancies, and it is rapidly progressing to be also efficacious against solid tumors.[1–3] To continue its development, it is necessary to optimize and standardize protocols for upscaling clinical cell manufacture.[4,5] To effectively treat a malignancy, a single dose of engineered T cells could require several hundreds of thousands of therapeutic patient-derived T cells, that must retain the desired phenotype and function to ensure the effectiveness of treatment.[6,7] To successfully expand T cells *ex vivo*, before or after the genetic modification, they are first artificially stimulated to imitate the *in vivo* function of antigen-presenting cells (APCs) to subsequently proliferate under immunological synapses.[2,8]

Different methods are employed in the clinic to activate and expand T cells for therapeutic purposes. The simplest method to achieve therapeutic T cells is the activation and expansion in suspension. However, researchers have also explored other alternatives such as including materials that can simulate APCs to activate and trigger T cell proliferation. As a result, various substrates classified in length scale as nano, micro, or macro-environment to activate and expand T cells *ex vivo* have been developed.[2,9–13] The inclusion of rigid commercial substrates, such as the colloidal polymeric nano-matrix TransACT[8,9,14] and micro-magnetic Dynabeads[8,9,13] are the most used methods of activation and subsequent expansion of T cells in suspension. T cell development occurs in lymphoid tissues, primarily in the thymus, which are heterogeneous, complex, and dense structures with specific mechanical and chemical characteristics, such as stiffness between 0.1 and 3 kPa.[15–17] The 3D cellular environment was demonstrated to influence multiple cell functions, such as activation, gene expression, proliferation, migration, morphology, and differentiation.[18–23] Therefore, using suspension culture, or nano- and micro-scale scaffolds could yield expanded T cells that do not retain the desired therapeutic phenotype and function,[11] showing a reduced *in vivo* persistence and limited potency.[24] The primary setback of those artificial platforms is the partial recreation of the natural

[a]*Deparment of Chemical Engineering, University of Puerto Rico-Mayagüez, Road 108 Km. 1.0 Bo. Miradero. P.O. Box 9046, Mayagüez, 00681-9046, Puerto Rico, USA. E-mail: madeline.torres6@upr.edu; Tel: +1 787 832 4040 Ext. 2585*

[b]*Department of Biomedical Engineering, University of Wisconsin–Madison, Madison, Wisconsin, USA*

† Electronic supplementary information (ESI) available. See DOI: https://doi.org/10.1039/d4ra01968g

T cell environment due to the lack of an entire 3D system or their rigidity.[13,25] Moreover, the use of these platforms could be time-consuming and expensive, and the cell harvesting processes for downstream assays or applications, may require the use of specialized equipment that usually brings some drawbacks.[26]

An alternative to simulate, with higher precision, the physical properties of the T cell environment could be the use of 3D macro-scale substrates.[9,18,27] Indeed, some 3D macro-scale substrates have been used as artificial APCs in order to have continuous contact with T cells and enhance T cell activation and subsequent expansion.[8,15,16,25,28] Also, others have been used as implants to expand T cells and deliver them to the tumor site.[29–33] Both types of research included the evaluation of scaffold stiffness with artificial activation signals or used pre-activated T cells to study T cell behavior. These investigations revealed that T and chimeric antigen receptor (CAR)-T cells could proliferate, be encapsulated, and sense 3D solid environments. However, even those materials that possessed 3D environments, sometimes formed a layer in the bottom of the tissue culture plate, inducing cells to grow on top more like 2D instead of real 3D matrices. Also, the majority contain natural-based materials that could possess issues with variability in results that are common on these types of materials.[15,34]

For these reasons, this investigation proposed the use of a synthetic and thermo-responsive terpolymer material, previously developed in our laboratory,[35] as a macro-scale scaffold to culture T and CAR-T cells. The terpolymer material was composed of synthetic momoners to avoid issues carried by natural sources and it was specially designed to possess thermo-responsive properties to facilitate cell harvesting after encapsulation. Furthermore, this smart and non-cytotoxic hydrogel was proven to have several advantageous features for Jurkat T cell encapsulation and culture.[35] In this study, two thermo-responsive terpolymers with different mechanical properties (0.5 ± 0.2 kPa 17 ± 2.5 kPa) were investigated. The selected stiffness values were based on mimicking some biologically relevant stiffnesses T cells face, while traveling to secondary lymphoid organs and peripheral tissues.[32,36] It was hypothesized that T and CAR-T cell encapsulation within a macro-scale solid matrix would promote cell expansion by simulating the mechanical environment of lymphoid tissues, while providing ease of recovery. Results showed that the matrix mechanical properties potentially influenced the Pan-T and CAR-T cell behavior by improving cell viability and expansion in softer scaffolds, achieving similar results to the control suspension culture. Within the softer terpolymer, Pan-T cells produced a significant number of cells that also possessed phenotypic profiles suitable for therapeutic treatments. Encapsulated CAR-T cells also showed promising features by maintaining the CAR-T cell content and increasing the therapeutic memory CAR-T cell subpopulation. In particular, these results demonstrated that the encapsulation process within thermo-responsive terpolymer scaffolds supported T cell activation and maintenance of several memory and effector subpopulations, while providing easy recovery with minimal mechanical manipulation. The measurement of cytokines and lactate production also supported this statement. Together, these results suggested that the evaluated thermo-responsive hydrogels are promising 3D synthetic scaffolds for *in vitro* T cell expansion and could contribute to the cell manufacturing process by adding a valuable tool to help improve T cell immunotherapy.

2. Methodology

2.1. Synthetic scaffolds

As detailed elsewhere, the thermo-responsive terpolymer samples were synthesized, characterized, washed, and sterilized for cell culture applications as described elsewhere.[35] Terpolymers are a polymerization of *N*-isopropylacrylamide (NiPAAm), 4-vinylphenylboronic acid (4-VPBA), and polyethylene glycol monomethyl ether monomethacrylate (PEGMMA) of 400 g mol^{-1} monomers.

2.1.1. Terpolymer preparation. Samples were synthesized by free radical polymerization method for 24 hours using anhydrous ethanol and 2,2′-azobis(2-methylpropionitrile) (AIBN) as the solvent and initiator, respectively. After that, petroleum ether was used as a precipitant. Samples were dried until complete liquid evaporation, recovered, and washed for unreacted monomers elimination with D.I. water by thermo-precipitation. Once washed samples were characterized with thermal and mechanical techniques to corroborate the parameters previously published.

2.1.2. Sample sterilization. After washing, the terpolymer samples were sterilized by filtration using a gamma sterile syringe with a hydrophilic syringe filter of 0.22 μm pore size and 33 mm diameter of polyether sulfone (PES) membrane (Millipore Sigma, St. Louis, MO, USA). Briefly, dried terpolymer samples were weighed and dissolved in fresh cell culture medium to form a 15 wt% solution. In a laminar flow hood, using a plastic sterilized syringe, the terpolymer solution was filtered and stored on a sterile centrifuge tube for future use in cell culture.

2.2. Cell culture

Frozen Human Peripheral Blood Pan T cells isolated with negative immunomagnetic separation were purchased from StemCell Technologies (StemCell Technologies, Vancouver, BC, Canada). Non-viral CAR-T cells specifically targeting anti-GD2 were manufactured as described elsewhere[37] at the University of Wisconsin Madison and kindly sent to us. CAR-T cells were cryopreserved at 10 M cells per vial in FBS at 10% DMSO. T cells were activated for 48 hours using 25 μl ml^{-1} of ImmunoCult Human CD3/CD28/CD2 T Cell Activator (StemCell Technologies, Vancouver, BC, Canada) at a density of 1 M cells per mL. The serum- and xeno-free ImmunoCult™-XF T Cell Expansion Medium (StemCell Technologies, Vancouver, BC, Canada) in the presence of 500 U mL^{-1} of Human Recombinant IL-2 (PeproTech, Cranbury, NJ, USA) was used as a complete medium to maintain the cells. Cell types were maintained and cultured in 25 cm^2 culture flasks at 1 M cells per ml density and cell culture conditions, 37 °C and 5% CO_2.

2.3. Cell encapsulation

Cells were encapsulated in 96 well plates using the sandwich methodology previously described by Lizana-Vasquez *et al.*[35] Briefly, a polymer solution 15 wt% was prepared by mixing the appropriate amount of polymer and solubilized using culture media. This solution was further sterilized by filtration. A 7.5 wt% solution was prepared by diluting the previously sterilized 15 wt% solution. To create the terpolymer coating, a volume of 200 μL of terpolymer solution at 7.5 wt% was added to each well and incubated at 37 C for 3 h. cells were mixed with the terpolymer solution and were seeded on top of a terpolymer coating. Then, an additional 50 μL of terpolymer solution at 15 wt% was resuspended with 50 μL culture media containing cells to be gently seeded above the previously prepared polymer-coated well and incubated at cell culture conditions.

Terpolymer combinations 2:4:94_P400 and 4:12:84_P400 at 7.5 wt% concentration in cell culture media encapsulated Pan-T and CAR-T cells.

To encapsulate Pan-T cells, three end time points of incubation (5, 10, and 14 days) were set, seeding an amount of 50 000 Pan-T cells in flat bottom 96 well plates (Thermo Fisher Scientific, Waltham, MA, USA) with a total volume of 300 μL per well. CAR-T cells were encapsulated at the same conditions as Pan-T cells but only for 5 days, considering 150 000 cells per well. When 50 000 cells per well were employed, 3 wells were used to have an experimental replicate, while with 150 000 cells per well, one well was an experimental replicate.

2.4. Cell harvesting

At the desired time point, a volume of 150 μL of supernatant was removed and stored for cytokine and lactate analysis. Then, to harvest Pan-T and CAR-T cells, an amount of 150 μL of cool media (4 °C) was added to each well and rested for 15 minutes allowing it to turn liquid again. After resuspension, an amount of 200 μL sample was transferred to a 1.5 ml centrifuge tube, and 150 μL of cool media was added to wash the well. These processes were repeated one more time. For further analyses, cells were concentrated in 200 μL of cell media after centrifugation for 5 minutes at 300 g.

2.5. Cell viability

After cells were harvested from terpolymer matrices, they were maintained in a cell culture medium similar to the control suspension culture. The cell viability was determined by fluorescent live and dead discrimination with the ViaStain™ AO/PI Staining Solution (Nexcelom Bioscience LLC, Lawrence, MA, USA) in a 1 : 1 ratio. Cells with the AO/PI dye were placed in disposable hemocytometers and automatically counted using the Cellometer equipment Vision model (Nexcelom Bioscience LLC, Lawrence, MA, USA).

2.6. T cell expansion

The T cell fold expansion was calculated with the relation between the live cell numbers at a specific time and the cell numbers at the initial time of the experiment. Cells stained with ViaStain™ AO/PI Staining Solution (Nexcelom Bioscience LLC, Lawrence, MA, USA) were automatically counted with the Cellometer equipment Vision model (Nexcelom Bioscience LLC, Lawrence, MA, USA).

2.7. Fluorescent cell staining

Live cell staining of the nucleus (blue), live cells (green), and dead cells (red) was performed using a cocktail of 150 μL of Hoechst (0.033 mM) (Invitrogen, Waltham, MA, USA), Calcein AM (0.002 mM) (BD Bioscience, Franklin Lakes, NY, USA), and Ethidium Homodimer (0.003 mM) (Sigma Aldrich, St. Louis, MO, USA) staining solutions in PBS, respectively. After adding the dye cocktail, three hours of incubation was grand to allow the Calcein AM stain to act. Images were obtained with a confocal microscope Olympus IX83 (Center Valley, PA, USA) with 3i Spinning Disk Confocal Imaging.

2.8. Flow cytometry

Changes in T cell phenotype by flow cytometry were performed to analyze activation and memory surface markers before and after T cell encapsulation using BD Accuri C6 Plus equipment (BD Bioscience, Franklin Lakes, NY, USA). Three and four multicolor flow cytometry panels were employed to study the T cell phenotype changes. Zombie NIR fixable cell viability dye (BioLegend, San Diego, CA, USA) was used to discriminate the dead cell population in both panels. To identify the activated T cell populations, APC-CD8, PE-CD69, and Kiravia blue HLA-DR labeled antibodies (BioLegend, San Diego, CA, USA) were employed. Similar to the activation panel, the memory panel also included APC-CD8 along with FITC-CD45RA labeled antibody (BioLegend, San Diego, CA, USA). In both panels, labeled antibodies were employed according to the manufacturer's instructions at 5 μl antibodies per 1 M cells in a 100 μL sample. Moreover, the CAR content of the T cell population was identified using 400 ng/10^6 T cells of 1A7 anti-14G2a idiotype antibody (Absolute Antibody, Boston, MA, USA) conjugated with APC Conjugation Kit – Lightning-Link (Abcam, Waltham, MA, USA). The 1A7 anti-14G2a idiotype antibody was employed along with FITC-CD8 labeled antibody to form 3 panels with PE-CD45RA, PE-CD45RO, and PE-HLADR (BioLegend, San Diego, CA, USA) for the CAR-cell phenotype characterization.

2.9. Cytokine secretion profile

The study was performed using Bio-Plex Pro Human Immunotherapy Panel, 20-Plex, according to the manufacturer's protocol and read in a Bio-Plex 200 Luminex System (Bio-Rad, Hercules, CA, USA). The following cytokines were measured: GM-CSF, IFN-γ, IL-2, IL-4, IL-5, IL-6, IL-8, IL-10, IL-13, IL-17A, TNF-α, IL-7, IL-15, IL-18, IP-10, MCP-1, MIG, MIP-1α, MIP-1β, RANTES. Cell medium samples were collected before cell harvesting on day 5 after encapsulation and immediately stored at −80 °C. On the day of the assay, samples were thawed and diluted at a 2 : 1 ratio in cell medium, which was also used as a baseline of the manufacturer protocol. From the dilution, 50 μL was used to perform all measurements. Values were normalized with the total number of cells counted at media collection.

2.10. Lactate production

Lactate production was measured using the bioluminescence Lactate-Glo Assay (Promega, Madison, MI, USA). Cell medium samples were collected before cell harvesting on day 5 after encapsulation and immediately stored at −80 °C. The sample medium was diluted in PBS in a 1 : 1200 ratio before performing the experiment according to the manufacturer's protocol and the luminescence was read in a Tecan Infinite 200 Pro M Plex Microplate Reade (Tecan Group Ltd, Männedorf, Switzerland). Values were normalized with the total number of cells counted when the sample was recovered.

2.11. Statistical analysis

Unless otherwise stated, two-way ANOVA with Tukey multi-comparison test was employed to identify significant comparisons between the 2 stiffness matrices and the suspension control. These studies were performed in GraphPad Prism, version 9.0 (GraphPad, San Diego, CA, USA) using a 5% significance level.

3. Results and discussion

A tailored thermo-responsive terpolymer material previously characterized by our laboratory[35] was used in this study as an artificial 3D scaffold for T cell encapsulation and culture. This hydrogel was characterized by its capability of easily attaching and detaching cells, supporting cell proliferation, transparency, and 3D encapsulation of cells including Jurkat T cells.[35] Two terpolymer combinations composed of 2% 4-VPBA, 4% PEGMMA400, and 94% NiPAAm (henceforth named 2:4:94 P400), and 4% 4-VPBA, 12% PEGMMA400, and 84% NiPAAm (henceforth named 4:12:84 P400) were specially selected for this study. The combination of these monomer molar ratios yielded terpolymers that possessed thermal and mechanical properties suitable for T cell encapsulation. The thermo-responsive terpolymer samples, whose mechanical characteristics are detailed in Table 1, were prepared and described elsewhere[35] and used for the encapsulation studies of Pan-T and CAR-T cells. This smart terpolymer hydrogel provided the opportunity to easily recover encapsulated cells by reducing the system temperature, which minimized the use of mechanical manipulation. Briefly, culture plates were taken out of incubation at 37 °C at the desired time point. Then they were incubated for 20 minutes with cold cell media (4 °C) to help the polymer change to liquid form, and gently harvest the cells. Cell harvesting from thermo-responsive terpolymer scaffolds was previously demonstrated with different cell lines,[35] and it was corroborated with Pan-T and CAR-T cells.

Table 1 Average results and standard deviation (SD) of thermo-responsive terpolymers Elastic Modulus. The size of the samples was $n = 6$

Properties G′@37 °C	2:4:94 P400	4:12:84 P400
Elastic modulus in D.I water[35]	17.8 ± 2.5 kPa	0.5 ± 0.2 kPa
Elastic modulus in T cell medium	16.7 ± 5.8 kPa	1.0 ± 0.3 kPa

3.1. Cell viability and expansion

To contribute to the manufacturing process of therapeutic CAR-T cells, different T cell lines were used to evaluate the thermo-responsive terpolymer matrix as a synthetic platform to support the proper T cell culture, before or after genetic modification. Usually, CAR-T cells products are manufactured from peripheral blood mononuclear cells (PBMC) isolated T cells. Therefore, commercially frozen naïve Pan-T cells from two donors were used. The biocompatibility of the material and the effect of the encapsulation process within terpolymers as a function of time with three endpoints of culture (5, 10, and 14 days) were investigated. The term "Pan T cells" is commercially used to describe the total T cell population, composed mostly of CD3+ T cells, regulatory T cells, and other subtypes.[38,39]

The traditional method of producing CAR-T cells with highly efficient gene transduction uses viral vectors, which carries several significant drawbacks related to patient safety and manufacturing practicality that could generate devastating hazards to patients.[40–42] To overcome these limitations, non-viral transfection techniques to insert CAR genes into T cells more efficiently and safely have been explored, including the revolutionized genome editing technology CRISPR/Cas9.[43,44] In a recent study using this technology, the generation, characterization, and evaluation of virus-free CAR-T cells to issue GD2 target-specific cancer cells have demonstrated encouraging results *in vitro* and *in vivo*.[37] Therefore, after testing Pan-T cells, frozen virus-free anti-GD2 CAR-T cells[37] with different CAR% from three donors were evaluated within terpolymers for 5 days of encapsulation, as they were already cultured before freezing. The viability of these T cell lines upon thawing is detailed in Table 2.

It was previously observed that T cell viability was affected by the activation process since T cells only become functional when stimulated and decide to become effector cells or anergize to maintain immune balance.[45,46] In this study, after artificial stimulation in suspension culture, the Pan-T cell viability was reduced from 97.4% to 82.3%, while CAR-T cells reduced their viability from 60.8% to 36.7%, 55.5% to 42.6%, and 60.8% to 28.1% for donors 1, 2, and 3 respectively. At this point, Pan-T and CAR-T cells were encapsulated and cultured in suspension for the corresponding time.

Table 2 Viability average results and standard deviation (SD) of T cell samples cultured in suspension. The size of the samples (biological replicates) was $n = 3$

T Cell sample	Viability after thawing (%)	Viability prior to encapsulation (%)
Pan-T cells	97.4 ± 1.4	82.3 ± 3.1
CAR-T cells donor 1 (50% CAR)	60.8 ± 7.0	36.7 ± 6.2
CAR-T cells donor 2 (35% CAR)	55.5 ± 2.8	42.6 ± 4.1
CAR-T cells donor 3 (10% CAR)	60.8 ± 1.3	28.1 ± 3.5

Once Pan-T and CAR-T cells were artificially stimulated for 48 hours, they were seeded and encapsulated within two thermo-responsive terpolymer matrix stiffness using the sandwich method previously described.[35] Images depicted in Fig. 1 illustrate that the encapsulation process did not affect the morphology of Pan-T or anti-GD2 CAR-T cells, and they were able to migrate and form clusters. T cells agglomerated when encapsulated in both matrices, but more easily in the softer scaffold. Usually, naïve T cells remain as single cells, but when activated, their size increases and forms clusters.[12,25,30,47] Therefore, the agglomeration of T cells observed in Fig. 1 was expected, and it was previously observed by others.[8,25,30] Nevertheless, not all the cells achieved activation after stimulation, so they remained as single cells, some of them died, and others remained naïve.[12,30] Fig. 1 also depicted that encapsulation within the softer or stiffer thermo-responsive terpolymer matrices did not interfere with the sequential behavior of T cells as a result of the activation process.

Fig. 2B illustrates Pan-T and CAR-T cell viability post-encapsulation. Pan-T cell viability was higher than 50% post 5 days of culture in all conditions. The viability achieved in control suspension culture was similar to encapsulated results within the softer terpolymer, but it was significantly higher than the stiffer matrix. Actually, Pan-T cell viability increased as a function of time until it reached 87% in suspension culture. Similar results were obtained in the softer matrix at the end of culture, whereas a 69% viability was obtained in the stiffer matrix. Analogously, as depicted in Fig. 2E, donor 1 CAR-T cells cultured in suspension improved the viability to 53%, which was higher than stiffer (23%) and softer (39%) encapsulated results. This behavior was only observed with donor 1 cells, since cell viability of donors 2 and 3 was enhanced when cells

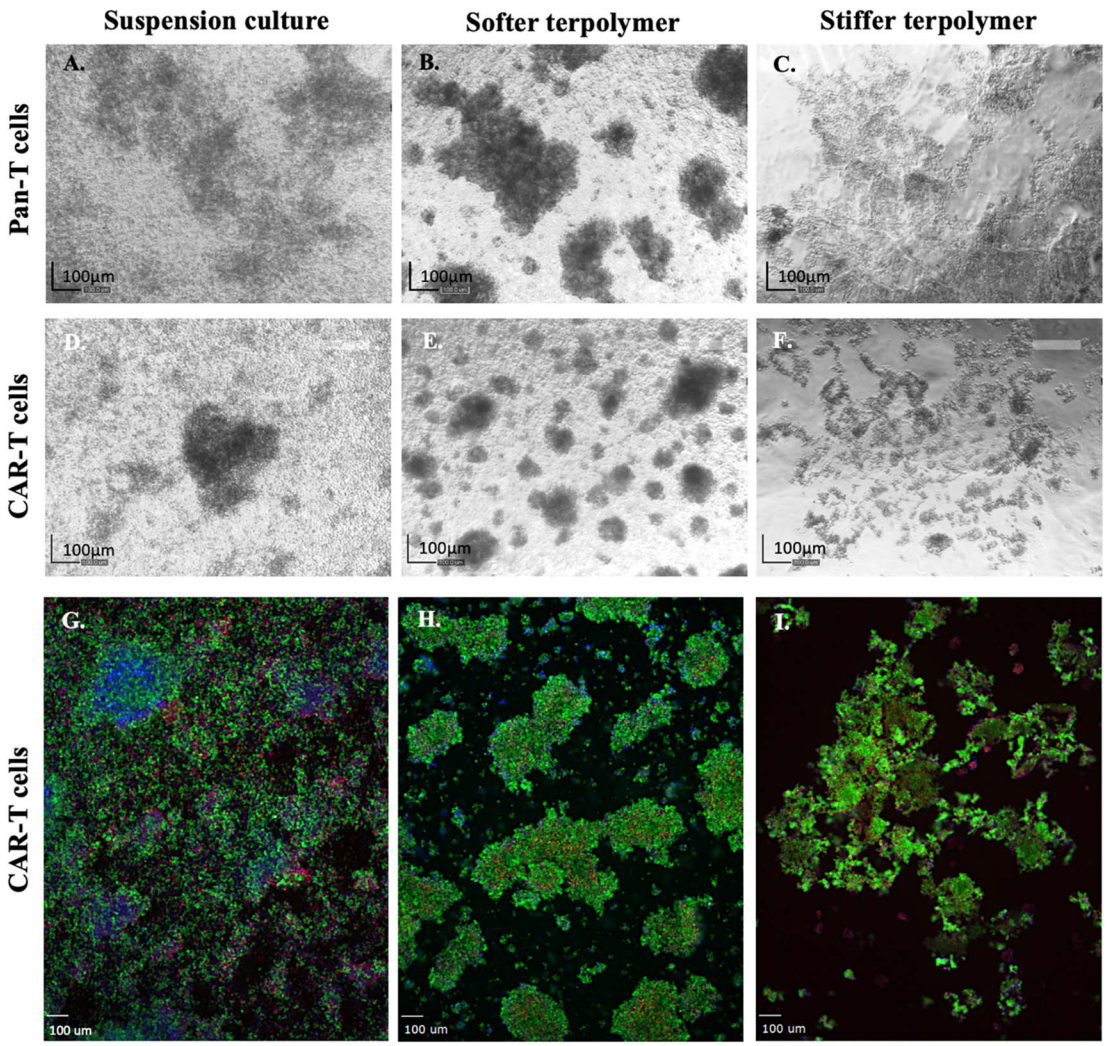

Fig. 1 Influence of scaffold stiffness in the Pan-T and anti-GD2 CAR-T cells behavior after 5 days of encapsulation and culture. Brightfield pictures A to C showed the culture of Pan-T cells in suspension (A) and encapsulated within 0.5 ± 0.2 kPa (B) and 17.8 ± 2.5 kPa (C) terpolymer matrices. Similarly, brightfield pictures D to F (donor 1 CAR-T cells) and fluorescent pictures G to I (donor 3 CAR-T cells) depicted the anti-GD2 CAR-T cells culture in suspension (D and G) and encapsulated within 0.5 ± 0.2 kPa (E and H) and 17.8 ± 2.5 kPa (F and I) terpolymers. In fluorescent pictures, the green (live cells), red (dead cells), and blue (cell nucleus) colors were stained with Calcein AM, Ethidium Homodimer, and Hoechst staining solutions, respectively.

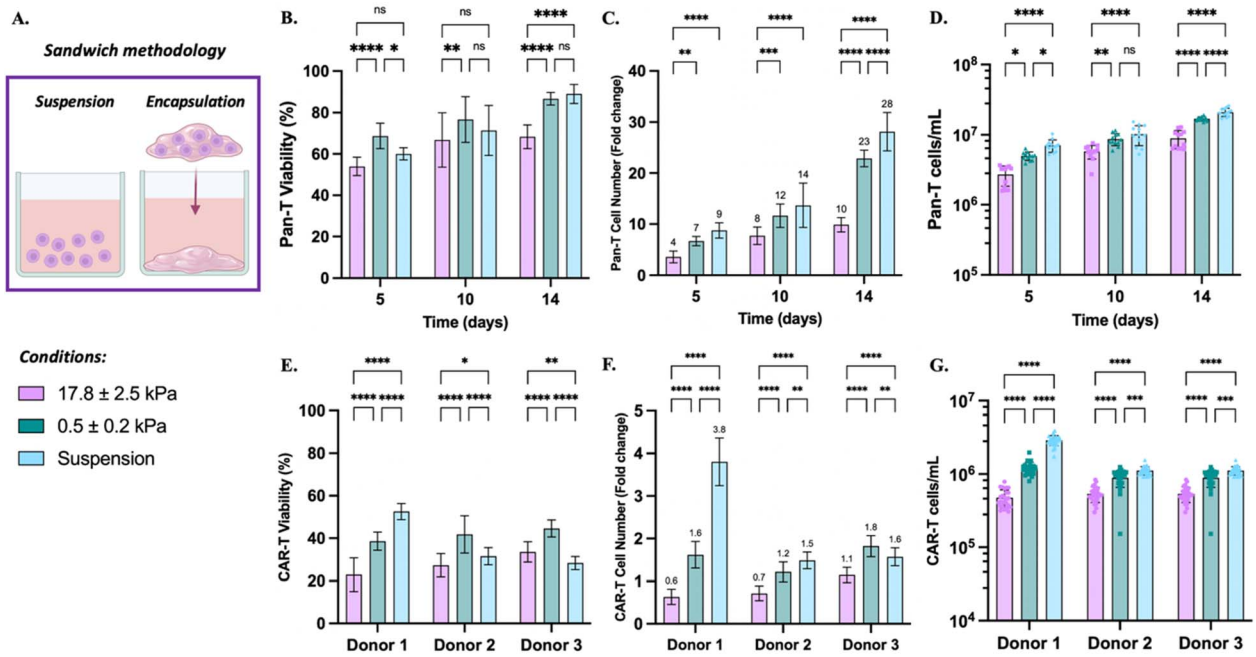

Fig. 2 Pan-T and CAR-T cell behavior within thermo-responsive terpolymer scaffolds over time. (A) Graphic representation of T cell encapsulation within terpolymer using the sandwich method. Control suspension: cells in the same working volume as the sandwich condition. Encapsulation: sandwich methodology formed by mixing cells with terpolymer and seeding them on top of a terpolymer coating. Comparison of cell viability (B and E), live fold expansion (C and F), and cell density (D and G). Pan-T cells were harvested after 5, 10, and 14 days of encapsulation within 2:4:94_P400 (17.8 ± 2.5 kPa) and 4:12:84_P400 (0.5 ± 0.2 kPa) terpolymer matrices, while CAR-T cells were harvested after 5 days. The results of encapsulated samples were compared with suspension culture as a control. Graphs show the means and S.D. values of $n = 18$ Pan-T cells and $n = 27$ CAR-T cells. Statistical significance was calculated with two-way ANOVA and Tukey multi-comparison test. *$P \leq 0.05$; **$p \leq 0.01$; ***$p \leq 0.001$; ****$p \leq 0.0001$.CAR-T cell content after encapsulation.

were encapsulated within the softer terpolymer. Previous studies demonstrated that T cells can identify and respond within minutes to environment stiffness through structural modifications in the cytoskeleton organization and transduced changes in gene expression.[48,49] Moreover, stiffer terpolymer matrix could result in lower diffusion coefficients for oxygen, nutrients, and metabolic by products, thus affecting viability.[50,51] Similar results, were observed with other stiff matrices used for T cell encapsulation, including chitosan[30]- and alginate-based[32] scaffolds.

Furthermore, it was demonstrated that the Pan-T cell population was able to increase over time after encapsulation, regardless of the value of the matrix stiffness (see Fig. 2C). The softer terpolymer stiffness influenced cell proliferation, obtaining better expansion compared to the stiffer terpolymer. After 5 days of encapsulation, cells expanded 7-fold within the softer terpolymer, which was statistically similar to the control in suspension culture. The same behavior was observed after 10 days of culture, but on day 14, the suspension culture achieved 28-fold, while the softer terpolymer matrix had a considerable Pan-T cell expansion of 23-fold. This last result was expected, as the cell expansion has an exponential tendency. Therefore, the small differences between the softer terpolymer and suspension culture in the early days were reflected with more intensity at the end of the culture. Nevertheless, the Pan-T cell expansion obtained within the thermo-responsive terpolymer matrices was higher than those reported with different materials for cell encapsulation. For instance, an alginate-base scaffold achieved 8.3-fold of CD8+ T cells after 7 days of encapsulation,[29] and a chitosan thermo-gel reached 7-fold of PBMC-derived T cells within 13 days of course.[30] Moreover, a 3D-polystyrene scaffold achieved an 11.1 expansion index, but the material used was a 2D scaffold instead of a 3D.[15] Regarding CAR-T cells, results from donors 1 and 2 suggested that encapsulated cells within the stiffer terpolymer were not able to grow after encapsulation, since fewer cells than the initial population were recovered. Donor 3 of the CAR-T cell results showed that the same number of live cells seeded were recovered at the end of the culture. However, encapsulated CAR-T cells within the softer terpolymer of the three donors were able to slightly grow after encapsulation. Suspension culture achieved a 3.9-fold expansion of donor 1 cells, while donors 2 and 3 just had 1.5- and 1.6-fold, respectively. Donor 3 cells showed a preference for growth within the softer matrix over suspension culture. It is important to remember that virus-free anti-GD2 CAR-T cell products came from fresh Pan-T cells that were genetically modified and cultured for 9 days before freezing,[37] then they were reactivated for terpolymer encapsulation experiments. Therefore, Pan-T and CAR-T cells were phenotypically different at the start of the experiment. That is why in this particular study, it was observed that CAR-T cell growth was slower than commercial Pan-T cells.

Table 3 CAR-T cell average content and standard deviation (SD) of anti-GD2 CAR-T cell samples after 5 days of culture. The size of the samples was $n = 27$ (3 biological replicates with 9 technical replicates)

T cell sample		17.8 ± 2.5 kPa	0.5 ± 0.2 kPa	Suspension
Donor 1	day 0	45.35 ± 2.98%	45.35 ± 2.98%	45.35 ± 2.98%
	day 5	48.14 ± 7.48%	44.11 ± 4.89%	30.11 ± 3.51%
Donor 2	day 0	36.99 ± 2.59%	36.99 ± 2.59%	36.99 ± 2.59%
	day 5	37.16 ± 5.15%	35.74 ± 5.70%	28.20 ± 6.08%
Donor 3	day 0	19.30 ± 3.10%	19.30 ± 3.10%	19.30 ± 3.10%
	day 5	23.69 ± 5.41%	20.92 ± 3.88%	21.28 ± 5.79%

Nevertheless, results have demonstrated that thermo-responsive terpolymer hydrogels were biocompatible and supported the survival and expansion of *in vitro* cultured T cells.

Virus-free anti-GD2+ CAR-T cells employed in this study were manufactured using CRISPR/Cas9 using recombinant Cas9 protein and nucleic acids.[37] They were frozen originally containing 50% (donor 1), 35% (donor 2), and 10% (donor 3) CAR+ population. After two days of activation, the CAR content observed in the live cell population was 45%, 40%, and 19%, for donors 1, 2, and 3 samples respectively, similar to the content labeled by the manufacturer. As Table 3 summarizes, suspension culture reduced the CAR+ content to 30% for donor 1. Interestingly, thermo-responsive terpolymer samples maintained the initial 45% CAR+. Since the suspension culture achieved a 3.8-fold expansion, the reduction in CAR content means that the growing T cell population may not contain the CAR expression. Likewise, the CAR+ content of donor 2 decreased to 28% when cells were cultured in suspension, while encapsulated cells maintained the initial CAR+. On the other hand, the CAR+ content of donor 3 was similar to the initial one without any significant difference between conditions.

3.2. Terpolymer effect on the cytotoxic CD8+ T cell subset

According to the supplier, the commercial naïve Pan-T cells used in this study had a mix of CD3+ T cells, and some γδ T cell subsets.[52] The CD3+ T cell subpopulations, T cytotoxic cells (CD8+) and T helper cells (CD4+), play an essential role in the T cell immunotherapy response against pathogens and viruses.[53,54] Similarly, anti-GD2+ CAR-T cells employed were manufactured from T cells isolated from peripheral blood mononuclear cells (PBMC), mostly CD4+ and CD8+ T cells.[37] The CD4+/CD8+ ratio is an important metric in CAR-T cell infusion products,[55–58] therefore we studied if the terpolymer significantly affected the percent of CD8+ T cells.

As depicted in Fig. 3B, after 5 days of culture the CD8+ subpopulation of Pan-T cells increased from an average of 37% to 50% in all conditions including suspension control. After that, the CD8+ subpopulation continued to increase in all conditions, but more easily in the suspension culture. Still, results did not show that the terpolymer matrix substantially affected the CD8+ population compared to the suspension control.

Furthermore, as illustrated in Fig. 3C, results showed that the terpolymer did not affect the CD8+ population compared to the suspension control. The differences in CD8+ expression of anti-GD2 CAR-T cell samples are typical, since the CD4+ and CD8+ subpopulations in humans vary greatly from donor to donor.[59–62]

Previous studies using macro-scale matrices have also observed changes in CD8+ subpopulation after T cell encapsulation and culture. For instance, Monette *et al.* reported the preference of CD8+ subpopulation to grow in a 3.9 kPa chitosan-base matrix, achieving a 65 to 75% expression.[30] That matrix was highly porous, which more likely helped to increase the gas diffusion and nutrient exchange. Similarly, the stiffer and the softer thermo-responsive terpolymer matrices allowed the expression of CD8+ Pan-T cell population to increase from 37% (pre-encapsulation) to 50% and 58%, respectively. Also, Cheung *et.al.* observed an increase in the CD8+ population when using bilipid-mesoporous silica micro-rods, which varied according to the formulation, but they achieved a high expression of CD8+ (almost 95%).[25] In that study, the commercial Dynabeads were

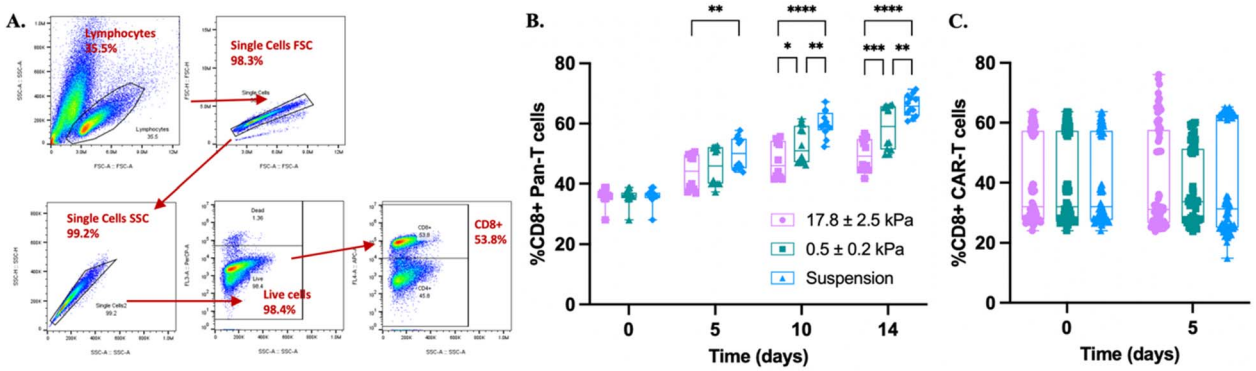

Fig. 3 Cytotoxic CD8+ T cell population of Pan-T and CAR-T cells. (A) Cells were gated for lymphocytes, singlets, and live cells before determining the CD8+ populations. Graphics show the flow cytometry results of the CD8+ population from the Pan-T (B), anti-GD2 CAR-T (C) cell samples. Day 0 showed the characteristic of cells after 2 days of stimulation when the encapsulation began. The results of encapsulated samples were compared with suspension culture as a control. Graphs show the means and S.D. values of $n = 18$ and $n = 27$ for Pan-T and CAR-T cells, respectively. Significance was determined by two-way ANOVA and Tukey multi-comparison test; *$p \leq 0.05$; **$p \leq 0.01$; ***$p \leq 0.001$; ****$p \leq 0.0001$.

used as control, which preferably expand CD4+ over CD8+ T cell fraction. For therapeutic purposes, both cell types, helper CD4+ and cytotoxic CD8+ T cells, are essential in cell immunotherapy. The increase in the cytotoxic CD8+ subpopulation is favorable for obtaining a good cytotoxic response. Still, helper CD4+ T cells are also important to potentiate the CD8+ anti-tumor activity due to their cytokine release and ability to resist exhaustion.[11] That is why it was suggested to expand CD4+ and CD8+ subsets separately and then add them in defined proportions during the formulation of CAR-T cell products.[63] Considering the sum of CD8+ and CD4+ T cell populations as almost 100% of PBMCs derived CAR-T cell products,[58,64] Fig. 3B showed that both T cell subtypes grow approximately in a 1 : 1 ratio within the softer terpolymer, which is very positive from the therapeutic point of view.

3.3. Metabolic T cell behavior

Once naïve T cells were stimulated *in vitro*, various cellular modifications occurred, including metabolic and phenotype changes, that entailed effective autocrine and paracrine signaling.[8,11] Moreover, it is known that metabolic processes, such as glycolysis, influence the immune cell function.[65,66] Therefore, to study if the encapsulation within the terpolymer matrix could influence T cell behavior by generating metabolic changes, lactate production was measured from supernatants after 5 days of culture. Results depicted in Fig. 4 suggest a tendency to increase lactate production as the stiffness of the culture increased, which is clearly observed with Pan-T cells and donors 1 and 2 CAR-T cell samples. The presence of high lactate levels when cells were encapsulated could be a result of anaerobic glycolysis occasioned by a reduced oxygen presence due to the stiffness of the terpolymer matrices.[67] Nevertheless, it is also known that T cell subsets undergo different metabolic profiles according to their needs.[68] For instance, resting naïve and memory effector T cells primarily metabolize glucose to pyruvate in the presence of oxygen to produce NADH and then fuel ATP production. However, upon stimulation, memory effector T cells rapidly switch this metabolic reaction to glycolysis to achieve the increased energy and biosynthesis demanded by T cell activation and proliferation, causing a subsequent increase in lactate production.[49,69] Therefore, this increased lactate production when cells were encapsulated within the thermo-responsive terpolymer could be also caused by the presence of memory effector T cell fraction. Furthermore, the higher lactate presence using the terpolymer matrix is beneficial since physiologically, lactate is a waste metabolite product of glycolysis, but it also serves as a primary carbon fuel source for energy, gluconeogenesis, and autocrine, paracrine, and endocrine signaling.[65,70] Still, it is important to regulate high-lactate, low-glucose, and high-pH immunosuppressive environments, that impair cytotoxic and effector T cell glycolysis and functions required for proliferation and cytokine production.[66]

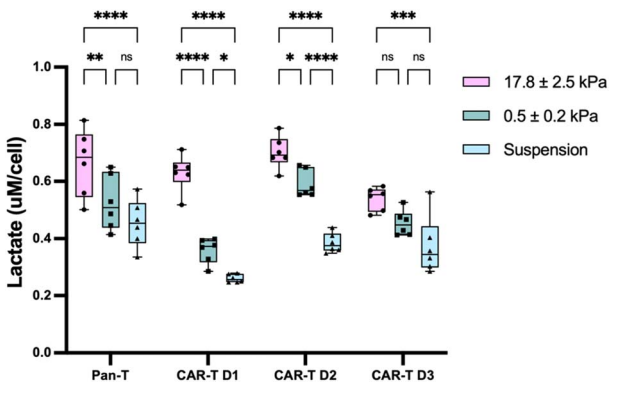

Fig. 4 Lactate production of Pan-T and CAR-T cells culture. Box plots show the means and SD of $n = 6$ samples after 5 days of culture. Statistical significance was calculated with two-way ANOVA and Tukey multi-comparison test. *$P \leq 0.05$; **$p \leq 0.01$; ***$p \leq 0.001$; ****$p \leq 0.0001$.

3.4. T cell phenotype

Even when stimulation is needed to achieve an adequate T cell expansion, it would be beneficial to ensure activation, but limit cell exhaustion to obtain significant cell numbers that are also therapeutic for cancer treatment. Stimulation changed the T cell phenotype from a resting stage to an active stage driving the T cell expansion and differentiation supported by cytokines secretion.[71,72] Therefore, antigens expressed on the cell membrane were identified by flow cytometry to study some T phenotypical changes due to the use of artificial stimulation and encapsulation process within a foreign solid matrix with different stiffness.

T cell activation occurs after a series of well-orchestrated occurrences following a suitable stimulation that triggers cell proliferation.[71,72] Usually, CD69, CD25, and HLA-DR antigen surface markers are used to identify the three activation stages, early, intermediate, and late phases, respectively. As observed in Fig. 5A, after two days of stimulation, when the encapsulation began, the CD69 antigen was expressed in 64% of Pan-T cells. After 5 days, the suspension culture and the softer matrix maintained the expression, while within the stiffer terpolymer matrix, it was reduced to 50%. On day 10, the CD69 expression was reduced in all conditions including control, particularly in encapsulated cells; while on day 14, the CD69 expression was further reduced to 30% in all tested conditions. Furthermore, Fig. 5B showed that as expected, only 13% of the Pan-T cell population was in the late activation phase of T cells (expressed by HLA-DR antigen) at the onset of encapsulation. The initial HLA-DR expression was robustly upregulated to 64% on day 5 of culture in all samples without statistical difference. After that, the HLA-DR expression was reduced in all conditions, but with more intensity within terpolymer matrix cultures. Synthetic biomaterials, such as the terpolymer samples, are not expected to promote T cell activation as a response, but alternative pathways such as mitogen can lead to T cell activation.[73] This possible extra activation, caused by the terpolymer matrices, could explain the accelerated reduction of the activation markers that achieved the plateau earlier than the control suspension culture. Furthermore, the upregulation of CD69 antigen expression may be followed by T cell proliferation and

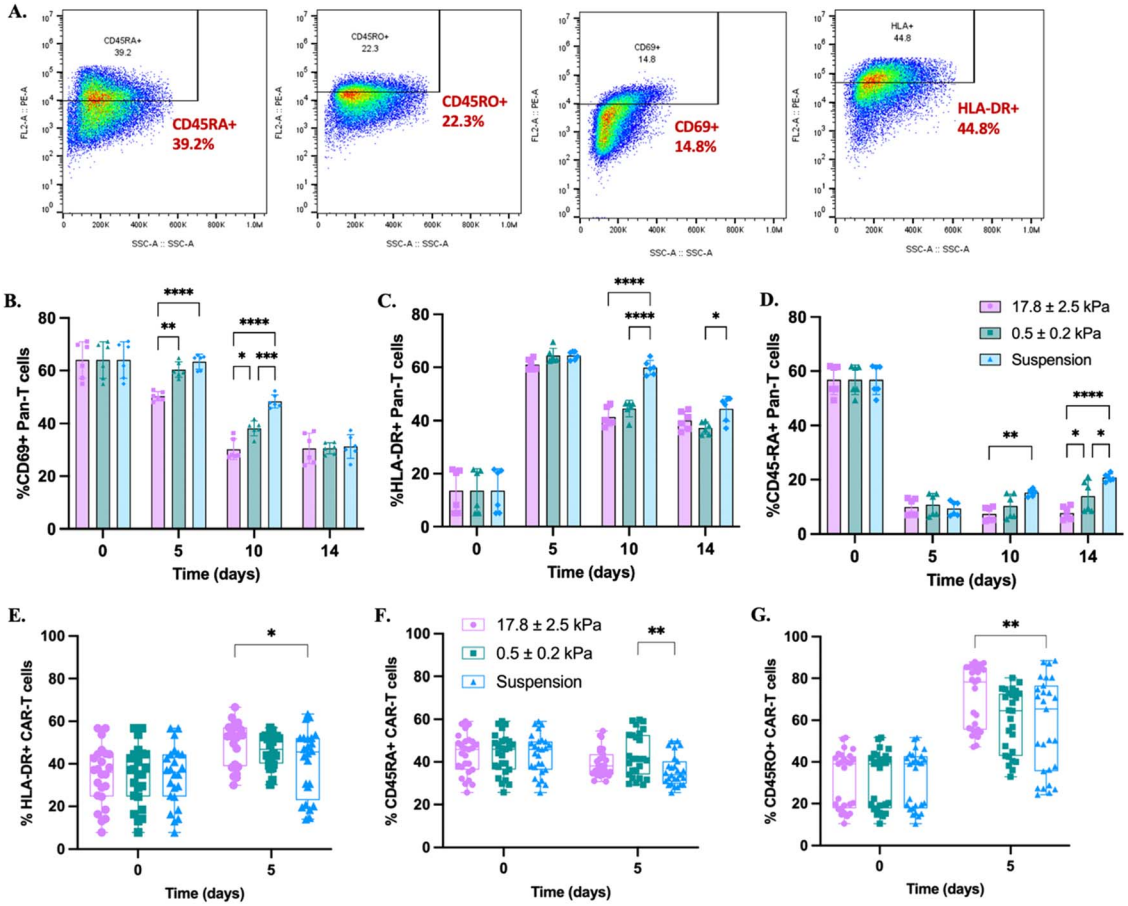

Fig. 5 Pan-T and CAR-T cell phenotype changes. (A) Cells were gated for lymphocytes, singlets, and live cells before determining the corresponding positive populations. Graphics show the expression results of CD69 (B), HLA-DR (C), and CD45RA (D) Pan-T cells after three encapsulation endpoints, 5, 10, and 14 days. Expression results of HLA-DR (E), CD45RA (F), and CD45RO (G) after 5 days of culturing CAR-T cells from three donors were also plotted. Day 0 showed the characteristic of cells after 2 days of stimulation when the encapsulation began. The results of encapsulated samples were compared with suspension culture as a control. Graphs show the means and S.D. values of $n = 9$ samples. Significance was determined by two-way ANOVA and Tukey multi-comparison test; *$p \leq 0.05$; **$p \leq 0.01$; ***$p \leq 0.001$; ****$p \leq 0.0001$.

increased cytokines secretion, which also boost T cell expansion.[74] That is why the T cell expansion on suspension culture was superior to encapsulated cells.

Regarding anti-GD2 CAR-T cell evaluation, Fig. 5D depicts that HLA-DR expression increased in all conditions. Anti-GD2 CAR-T cell batches were already activated during manufacturing, so the re-activation after thawing stimulated the cells again. Only the stiffer terpolymer matrix generated a significant change compared with the suspension culture.

Following stimulation, one characteristic phenotype change in T cells is the loss of expression of the CD45RA isoform and the increase of the CD45RO memory marker.[72,75–78] In this study, this particular behavior was observed by reducing CD45RA expression of Pan-T cells at a median value of 57% after 48 hours of activation (day 0). As is shown in Fig. 5C, the Pan-T cell CD45RA expression drastically decreased to 10% after 5 days of encapsulation in all conditions including control. Therefore, after encapsulation within thermo-responsive terpolymer matrices, naïve Pan-T cells continued their differentiation to memory and effector stages. The CD45RA population in the control suspension culture increased over time, reaching more expression than encapsulated cells. Encapsulated cells within the stiffer matrix kept constant the CD45RA expression along the three endpoint times, while within the softer terpolymer, it increased to 14% at the end of culture. After activation, naïve T cells that characteristically expressed CD45RA isoform, start their differentiation process to obtain memory functions and be therapeutically active, possessing self-replication and long-term immunity. But, at the end of the memory stage, T cells enter the effector stage, where they generally re-express the CD45RA isoform, then T cells reach exhaustion and undergo apoptosis.[62,79,80] Thus, at the end of culture, the effector memory differentiation stage is expressed in suspended cells and encapsulated cells within the softer matrix.

Fig. 5E illustrates the presence of CD45RA isoform in anti-GD2 CAR-T cells, which was reduced in all conditions including control, except on encapsulated cells within the softer terpolymer matrix. Also, Fig. 5F shows that CD45RO isoform increased in all conditions with a higher expression within the stiffer matrix. As the CD45RA isoform is lost after activation, the CD45RO isoform increased by the presence of primed/memory cells.[40,53–56] It could also be the case that CAR-T cells expressed

both isoforms as was previously reported by Mueller *et al.*, which is an indication of a transitional cell state.[37] They also reported that anti-GD2 CAR-T cells expressed high levels of CD45RO isoform before freezing. Thermo-responsive terpolymer matrices maintained a large CD45RO+ population which is associated with the memory population with therapeutic characteristics.

The differentiation and rapid transition of encapsulated T cells during their activation phase could be the reason for the increase in lactate production since T cell subsets undergo different metabolic profiles according to their needs.[68] Therefore, our results of CD45 isoform expressions are consistent with higher glycolysis in the culture suggesting a higher memory effector T cell fraction when they were encapsulated within the thermo-responsive terpolymer. In summary, these flow cytometry results of T cell phenotype demonstrated that the encapsulation process within the thermo-responsive terpolymer matrices supported T cell activation and multiple T cell subpopulations relevant for adoptive T cell therapy.

3.5. Cytokine profile

T cells can communicate through the secretion of small proteins (cytokines) to send corresponding signals according to their needs and are crucial modulators of inflammation, producing to recruit, stimulate, and proliferate other immune cells as a response to pathogens and viruses.[54,81,82] Therefore, 20 cytokines typically associated with the immunophenotyping response including interleukins (IL), chemokines, interferons, and tumor necrosis factors (TNF) were analyzed to profile T cell cytokine secretion. Fig. 6 depicts the cytokine results divided according to their immune response. Chemokine secretion results are plotted in ESI Fig. S1.†

Most of the studied cytokines of Pan-T cell culture did not show significant differences in results except for adaptive immune cytokine IL-14, and pro-inflammatory cytokines IL-17 and IL-18, where the stiffer matrix culture promoted more secretion. Cytokine results of anti-GD2 CAR-T cells related to adaptive immunity (IL-4, IL-5, IL-7, and IL-15), anti-inflammatory (IL-10), pro-inflammatory response (IL-6, IL-17, IL-18, and TNF-α), and chemokine (MIP-1α and RANTES) showed a tendency to increase with the presence of the stiffer terpolymer. This increment in cytokine secretion could be related to lactate production and the potential presence of higher memory effector T cell fraction when they were encapsulated within the thermo-responsive terpolymer. Furthermore, the physical pressure that the matrix stiffness is generating on

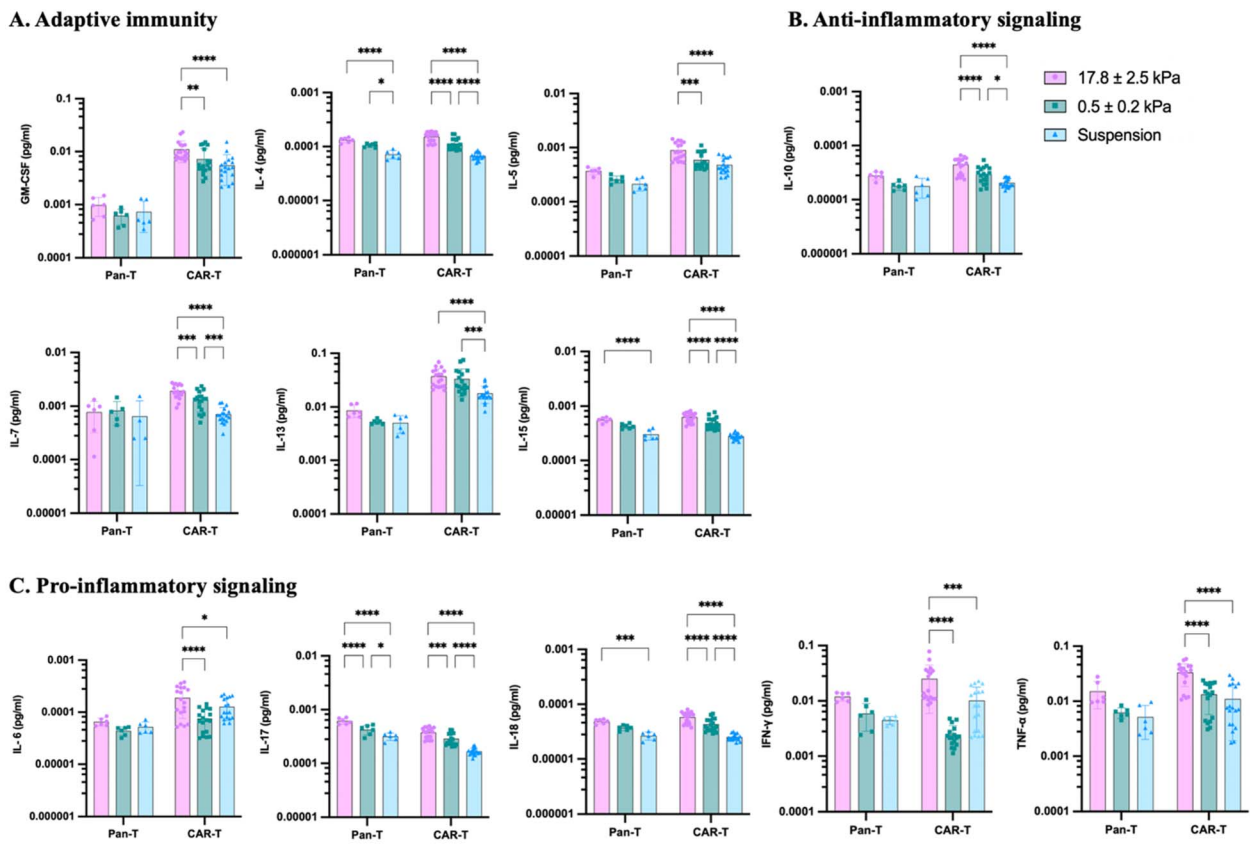

Fig. 6 Pan-T and anti-GD2 CAR-T cell cytokine secretion. Graphics depicted the expression of 12 cytokines classified by their immune response. (A) GM-CSF, IL-4, IL-5, IL-7, IL-13, and IL-15 are cytokines related to the adaptive immune response. The anti-inflammatory response was observed with the expression of IL-10 cytokine (B), while the pro-inflammatory response with IL-5, IL-17, IL-18, IFN-g, and TNF-a cytokines (C). Bars show the means and S.D. values of $n = 6$ samples for Pan-T cells and $n = 18$ for CAR-T cells. Statistical significance was calculated with two-way ANOVA and Tukey multi-comparison test. *$P \leq 0.05$; **$p \leq 0.01$; ***$p \leq 0.001$; ****$p \leq 0.0001$.

the T cell behavior could cause higher cytokine production, since mechanical forces also play an important role in T cell activation.[83] For instance, it has been demonstrated that T cells can identify and respond to the stiffness of the environment within minutes.[48] Moreover, results showed that CAR-T cells produced high levels of GM-CSF, IFN-γ, IL-8, IL-13, IP-10, MCP-1, RANTES, and TNF-α. This behavior was also observed with cytokines IL-8, IL-13, IFN-γ, and TNF-α on day 9 of CAR-T cell manufacturing as reported by Mueller *et al.*[37] In general, our results demonstrated that all cultured T cells, encapsulated and suspended, produced cytokines and chemokines signals related to human immunotherapy responses.

4. Conclusion

A novel, synthetic, and thermo-responsive scaffold of two different stiffness (0.5 and 17.8 kPa) was tested in this study for *in vitro* T and CAR-T cell encapsulation and expansion. The thermo-sensitive and mechanical properties of terpolymer scaffolds ensured 3D cell encapsulation, monitoring, and easy cell harvesting for downstream analysis. Commercially available Pan-T cells and virus-free anti-GD2 CAR-T cells were encapsulated in 3D within the terpolymer scaffolds, demonstrating the feasibility of using this material as 3D macro-scale scaffolds for T cell culture. Encapsulated T cells in both thermo-responsive terpolymer combinations were able to grow and behave like suspension control, forming cell clusters after encapsulation. The biocompatibility of terpolymers and the effect of the encapsulation process were corroborated by automatic cell counting. Results after encapsulation of pre-activated Pan-T cells have demonstrated that cells can survive and proliferate within the terpolymer hydrogels with a preference for the softer matrix. It was confirmed that the stiffness of the thermo-responsive terpolymer matrix influences the T cell behavior. The cell expansion obtained with the soft terpolymer of 0.5 ± 0.2 kPa was superior to the stiffer terpolymer matrix of 17.8 ± 2.5 kPa. Furthermore, a considerable Pan-T cell expansion was reached within the softer terpolymer with a similar phenotype to the suspension culture, obtaining significant cell numbers with an adequate phenotypical characteristic that could be tested for therapeutic purposes. After encapsulation, naïve Pan-T cells continued their activation and differentiation to the memory and effector stages. Regarding the CAR-T cell culture, it was observed that cell viability decreased when encapsulated within the terpolymer matrices, and cells were able to slightly grow only within the softer terpolymer. Nevertheless, the CAR-T cell phenotype results of memory markers CD45RA and CD45RO were very promising. Furthermore, cytokine secretion and lactate production measurements from supernatants support the potential presence of memory effector T cell fraction and confirm cell activation, differentiation, and metabolic response when they are encapsulated within terpolymers. Encapsulated cells within the softer terpolymer behave similarly to the suspension control, so its use as a solid substrate for cell encapsulation and culture that facilitates cell harvesting and media changes could potentially offer an advantage in the large-scale cell manufacturing process. This study provided evidence that thermo-responsive terpolymer hydrogels could contribute to the cell manufacturing process by adding a valuable tool to help improve T cell immunotherapy, promising 3D synthetic scaffolds for *in vitro* T cell expansion. Moreover, the 0.5 ± 0.2 kPa terpolymer material could be suitable for culturing other immune cell types, such as natural killer (NK), dendritic, monocytes, and macrophages.

Conflicts of interest

There are no conflicts of interest to declare.

Acknowledgements

This research was sponsored by the Engineering Research Center on Cell Manufacturing Technologies (CMaT), which is supported by the National Science Foundation (NSF) grant number EEC-1648035. Anti-GD2 CAR-T cells were obtained from Dr Krishanu Saha's lab with the logistical support of Ross Schwartz. We acknowledge Dr Maribella Domenech's and Dr Aldo Acevedo's labs from the UPRM Chemical Engineering department for allowing us to use the cell counting fluorescent equipment and rheometer, respectively.

References

1 B. L. Levine, J. Miskin, K. Wonnacott and C. Keir, Global Manufacturing of CAR T Cell Therapy, *Mol. Ther.–Methods Clin. Dev.*, 2017, **4**, 92–101, DOI: **10.1016/j.omtm.2016.12.006**.

2 N. J. Piscopo, K. P. Mueller, A. Das, P. Hematti, W. L. Murphy, S. P. Palecek, C. M. Capitini and K. Saha, Bioengineering Solutions for Manufacturing Challenges in CAR T Cells, *Biotechnol. J.*, 2018, **13**(2), 1–10, DOI: **10.1002/biot.201700095**.

3 G. D. Lizana-Vasquez, M. Torres-Lugo, R. B. Dixon, J. D. Powderly and R. F. Warin, The application of autologous cancer immunotherapies in the age of memory-NK cells, *Front. Immunol.*, 2023, **14**, 1–20, DOI: **10.3389/fimmu.2023.1167666**.

4 Y. Ando, C. Mariano and K. Shen, Engineered in vitro tumor models for cell-based immunotherapy, *Acta Biomater.*, 2021, **132**, 345–359, DOI: **10.1016/j.actbio.2021.03.076**.

5 S. MacPherson, *et al.*, Clinically relevant T cell expansion media activate distinct metabolic programs uncoupled from cellular function, *Mol. Ther.–Methods Clin. Dev.*, 2022, **24**, 380–393, DOI: **10.1016/j.omtm.2022.02.004**.

6 S. Ghaffari, *et al.*, Optimizing interleukin-2 concentration, seeding density and bead-to-cell ratio of T-cell expansion for adoptive immunotherapy, *BMC Immunol.*, 2021, **22**(1), 1–9, DOI: **10.1186/s12865-021-00435-7**.

7 X. Liu and Y. Zhao, CRISPR/Cas9 genome editing: Fueling the revolution in cancer immunotherapy, *Curr. Res. Transl. Med.*, 2018, **66**(2), 39–42, DOI: **10.1016/j.retram.2018.04.003**.

8 D. K. Y. Zhang, A. S. Cheung and D. J. Mooney, Activation and expansion of human T cells using artificial antigen-

presenting cell scaffolds, *Nat. Protoc.*, 2020, **15**(3), 773–798, DOI: 10.1038/s41596-019-0249-0.

9 I. I. Cardle, E. L. Cheng, M. C. Jensen and S. H. Pun, Biomaterials in chimeric antigen receptor T-cell process development, *Acc. Chem. Res.*, 2020, **53**(9), 1724–1738, DOI: 10.1021/acs.accounts.0c00335.

10 R. A. Meyer, *et al.*, Biodegradable Nanoellipsoidal Artificial Antigen Presenting Cells for Antigen Specific T-Cell Activation, *Small*, 2015, **11**(13), 1519–1525, DOI: 10.1002/smll.201402369.

11 N. J. Dwarshuis, H. W. Song, A. Patel, T. Kotanchek and K. Roy, Functionalized microcarriers improve T cell manufacturing by facilitating migratory memory T cell production and increasing CD4/CD8 ratio, *bioRxiv*, 2019, p. 646760, DOI: 10.1101/646760.

12 H. Lin, *et al.*, Automated Expansion of Primary Human T Cells in Scalable and Cell-Friendly Hydrogel Microtubes for Adoptive Immunotherapy, *Adv. Healthcare Mater.*, 2018, **7**(15), 1–13, DOI: 10.1002/adhm.201701297.

13 L. H. Lambert, *et al.*, Improving T Cell Expansion with a Soft Touch, *Nano Lett.*, 2017, **17**(2), 821–826, DOI: 10.1021/acs.nanolett.6b04071.

14 A. Casati, *et al.*, Clinical-scale selection and viral transduction of human naïve and central memory CD8+ T cells for adoptive cell therapy of cancer patients, *Cancer Immunol., Immunother.*, 2013, **62**(10), 1563–1573, DOI: 10.1007/s00262-013-1459-x.

15 E. Pérez Del Río, M. Martinez Miguel, J. Veciana, I. Ratera and J. Guasch, Artificial 3D Culture Systems for T Cell Expansion, *ACS Omega*, 2018, **3**(5), 5273–5280, DOI: 10.1021/acsomega.8b00521.

16 J. W. Hickey, *et al.*, Engineering an Artificial T-Cell Stimulating Matrix for Immunotherapy, *Adv. Mater.*, 2019, **31**(23), 1–14, DOI: 10.1002/adma.201807359.

17 B. V Kumar, T. J. Connors and D. L. Farber, Human T Cell Development, Localization, and Function throughout Life, *Immunity*, 2018, **48**(2), 202–213, DOI: 10.1016/j.immuni.2018.01.007.

18 K. Adu-Berchie and D. J. Mooney, Biomaterials as local niches for immunomodulation, *Acc. Chem. Res.*, 2020, **53**(9), 1749–1760, DOI: 10.1021/acs.accounts.0c00341.

19 R. S. O'Connor, *et al.*, Substrate Rigidity Regulates Human T Cell Activation and Proliferation, *J. Immunol.*, 2012, **189**(3), 1330–1339, DOI: 10.4049/jimmunol.1102757.

20 L. Chen, C. Yan and Z. Zheng, Functional polymer surfaces for controlling cell behaviors, *Mater. Today*, 2018, **21**(1), 38–59, DOI: 10.1016/j.mattod.2017.07.002.

21 O. Chaudhuri, Viscoelastic hydrogels for 3D cell culture, *Biomater. Sci.*, 2017, **5**(8), 1480–1490, DOI: 10.1039/c7bm00261k.

22 S. F. B. Mennens, M. Bolomini-Vittori, J. Weiden, B. Joosten, A. Cambi and K. Van Den Dries, Substrate stiffness influences phenotype and function of human antigen-presenting dendritic cells, *Sci. Rep.*, 2017, **7**(1), 1–14, DOI: 10.1038/s41598-017-17787-z.

23 R. Chen, L. Li, L. Feng, Y. Luo, M. Xu, K. Leong and R. Yao, Biomaterial-assisted scalable cell production for cell therapy, *Biomaterials*, 2020, **230**, 119627, DOI: 10.1016/j.biomaterials.2019.119627.

24 R. Hammink, *et al.*, Semiflexible Immunobrushes Induce Enhanced T Cell Activation and Expansion, *ACS Appl. Mater. Interfaces*, 2021, **13**(14), 16007–16018, DOI: 10.1021/acsami.0c21994.

25 A. S. Cheung, D. K. Y. Zhang, S. T. Koshy and D. J. Mooney, Scaffolds that mimic antigen-presenting cells enable ex vivo expansion of primary T cells, *Nat. Biotechnol.*, 2018, **36**(2), 160–169, DOI: 10.1038/nbt.4047.

26 M. Frenea-Robin and J. Marchalot, Basic Principles and Recent Advances in Magnetic Cell Separation, *Magnetochemistry*, 2022, **8**(1), DOI: 10.3390/magnetochemistry8010011.

27 M. O. Dellacherie, B. R. Seo and D. J. Mooney, Macroscale biomaterials strategies for local immunomodulation, *Nat. Rev. Mater.*, 2019, **4**(6), 379–397, DOI: 10.1038/s41578-019-0106-3.

28 A. P. Dang, *et al.*, Enhanced Activation and Expansion of T Cells Using Mechanically Soft Elastomer Fibers, *Adv. Biosyst.*, 2018, **2**(2), 1–6, DOI: 10.1002/adbi.201700167.

29 S. B. Stephan, A. M. Taber, I. Jileaeva, E. P. Pegues, C. L. Sentman and M. T. Stephan, Biopolymer implants enhance the efficacy of adoptive T-cell therapy, *Nat. Biotechnol.*, 2015, **33**(1), 97–101, DOI: 10.1038/nbt.3104.

30 A. Monette, C. Ceccaldi, E. Assaad, S. Lerouge and R. Lapointe, Chitosan thermogels for local expansion and delivery of tumor-specific T lymphocytes towards enhanced cancer immunotherapies, *Biomaterials*, 2016, **75**, 237–249, DOI: 10.1016/j.biomaterials.2015.10.021.

31 J. Weiden, *et al.*, Injectable biomimetic hydrogels as tools for efficient T Cell expansion and delivery, *Front. Immunol.*, 2018, **9**, 1–15, DOI: 10.3389/fimmu.2018.02798.

32 F. S. Majedi, M. M. Hasani-Sadrabadi, T. J. Thauland, S. Li, L. S. Bouchard and M. J. Butte, T-cell activation is modulated by the 3D mechanical microenvironment, *Biomaterials*, 2020, **252**, 120058, DOI: 10.1016/j.biomaterials.2020.120058.

33 P. Agarwalla, *et al.*, Bioinstructive implantable scaffolds for rapid in vivo manufacture and release of CAR-T cells, *Nat. Biotechnol.*, 2022, **40**(8), 1250–1258, DOI: 10.1038/s41587-022-01245-x.

34 C. Wang, *et al.*, Matrix stiffness modulates patient-derived glioblastoma cell fates in three-dimensional hydrogels, *Tissue Eng., Part A*, 2021, **27**(5–6), 390–401, DOI: 10.1089/ten.tea.2020.0110.

35 G. D. Lizana-Vasquez, L. F. Arrieta-Viana, J. Mendez-Vega, A. Acevedo and M. Torres-Lugo, Synthetic Thermo-Responsive Terpolymers as Tunable Scaffolds for Cell Culture Applications, *Polymers*, 2022, **14**(20), DOI: 10.3390/polym14204379.

36 X. Zhang, *et al.*, Unraveling the mechanobiology of immune cells, *Curr. Opin. Biotechnol.*, 2020, **66**, 236–245, DOI: 10.1016/j.copbio.2020.09.004.

37 K. Mueller, N. Piscopo, M. Forsberg, L. Saraspe, A. Das, B. Russell, M. Smerchansky, D. Cappabianca, L. Shi, K. Shankar, L. Sarko, N. Khajanchi, N. Denne,

A. Ramamurthy, A. Ali, C. Lazzarotto, S. Tsai, C. Capitini and K. Saha, Production and characterization of virus-free, CRISPR-CAR T cells capable of inducing solid tumor regression, *J. Immunother. Cancer*, 2022, **10**(9), e004446, DOI: 10.1136/jitc-2021-004446.

38 Y. Pan, *et al.*, Athymic mice reveal a requirement for T-cell-microglia interactions in establishing a microenvironment supportive of Nf1 low-grade glioma growth, *Genes Dev.*, 2018, **32**(7–8), 491–496, DOI: 10.1101/gad.310797.117.

39 Y. Xie and E. S. Jaffe, How i Diagnose Angioimmunoblastic T-Cell Lymphoma, *Am. J. Clin. Pathol.*, 2021, **156**(1), 1–14, DOI: 10.1093/ajcp/aqab090.

40 N. J. Piscopo, *et al.*, Bioengineering Solutions for Manufacturing Challenges in CAR T Cells, *Biotechnol. J.*, 2018, **13**(2), 1–10, DOI: 10.1002/biot.201700095.

41 S. Hacein-Bey-Abina, *et al.*, Insertional oncogenesis in 4 patients after retrovirus-mediated gene therapy of SCID-X1, *J. Clin. Invest.*, 2008, **118**(9), 3132–3142, DOI: 10.1172/JCI35700.

42 M. Logun, *et al.*, Label-free in vitro assays predict the potency of anti-disialoganglioside chimeric antigen receptor T-cell products, *Cytotherapy*, 2023, 1–13, DOI: 10.1016/j.jcyt.2023.01.008.

43 F. A. Ran, P. D. Hsu, J. Wright, V. Agarwala, D. A. Scott and F. Zhang, Genome engineering using the CRISPR-Cas9 system, *Nat. Protoc.*, 2013, **8**(11), 2281–2308, DOI: 10.1038/nprot.2013.143.

44 P. D. Hsu, E. S. Lander and F. Zhang, Development and applications of CRISPR-Cas9 for genome engineering, *Cell*, 2014, **157**(6), 1262–1278, DOI: 10.1016/j.cell.2014.05.010.

45 Y. Zhan, E. M. Carrington, Y. Zhang, S. Heinzel and A. M. Lew, Life and death of activated T cells: How are they different from naïve T Cells?, *Front. Immunol.*, 2017, **8**, 1–9, DOI: 10.3389/fimmu.2017.01809.

46 R. Arakaki, A. Yamada, Y. Kudo, Y. Hayashi and N. Ishimaru, Mechanism of activation-induced cell death of T cells and regulation of FasL expression, *Crit. Rev. Immunol.*, 2014, **34**(4), 301–314, DOI: 10.1615/CritRevImmunol.2014009988.

47 B. Delalat, *et al.*, 3D printed lattices as an activation and expansion platform for T cell therapy, *Biomaterials*, 2017, **140**, 58–68, DOI: 10.1016/j.biomaterials.2017.05.009.

48 M. Aramesh, D. Stoycheva, L. Raaz and E. Klotzsch, Engineering T-cell activation for immunotherapy by mechanical forces, *Curr. Opin. Biomed. Eng.*, 2019, **10**, 134–141, DOI: 10.1016/j.cobme.2019.05.004.

49 J. A. Shyer, R. A. Flavell and W. Bailis, Metabolic signaling in T cells, *Cell Res.*, 2020, **30**(8), 649–659, DOI: 10.1038/s41422-020-0379-5.

50 F. V. Lavrentev, V. V. Shilovskikh, V. S. Alabusheva, V. Y. Yurova, A. A. Nikitina, S. A. Ulasevich and E. V. Skorb, Diffusion-Limited Processes in Hydrogels with Chosen Applications from Drug Delivery to Electronic Components, *Molecules*, 2023, **28**(15), 5931, DOI: 10.3390/molecules28155931.

51 T. Andersen, P. Auk-Emblem and M. Dornish, 3D Cell Culture in Alginate Hydrogels, *Microarrays*, 2015, **4**(2), 133–161, DOI: 10.3390/microarrays4020133.

52 STEMCELL Technology, Human Peripheral Blood Pan-T Cells, Frozen, 2023, Accessed: Nov. 07. [Online]. Available: https://www.stemcell.com/human-peripheral-blood-pan-t-cells-frozen.html.

53 B. Farhood, M. Najafi and K. Mortezaee, CD8+ cytotoxic T lymphocytes in cancer immunotherapy: A review, *J. Cell. Physiol.*, 2019, **234**(6), 8509–8521, DOI: 10.1002/jcp.27782.

54 M. D. Turner, B. Nedjai, T. Hurst and D. J. Pennington, Cytokines and chemokines: At the crossroads of cell signalling and inflammatory disease, *Biochim. Biophys. Acta Mol. Cell Res.*, 2014, **1843**(11), 2563–2582, DOI: 10.1016/j.bbamcr.2014.05.014.

55 D. Sommermeyer and *et al.*, *Accepted Article Preview : Published ahead of Advance Online Publication, No. August*, Nature Publishing Group, 2015. doi: DOI: 10.1038/leu.2015.247.

56 C. J. Turtle, *et al.*, CD19 CAR–T cells of defined CD4+:CD8+ composition in adult B cell ALL patients, *J. Clin. Invest.*, 2016, **126**(6), 2123–2138, DOI: 10.1172/JCI85309.

57 A. D. Fesnak, C. H. June and B. L. Levine, Engineered T cells: The promise and challenges of cancer immunotherapy, *Nat. Rev. Cancer*, 2016, **16**(9), 566–581, DOI: 10.1038/nrc.2016.97.

58 S. Stock, M. Schmitt and L. Sellner, Optimizing manufacturing protocols of chimeric antigen receptor t cells for improved anticancer immunotherapy, *Int. J. Mol. Sci.*, 2019, **20**(24), 6223, DOI: 10.3390/ijms20246223.

59 J. A. McBride and R. Striker, Imbalance in the game of T cells: What can the CD4/CD8 T-cell ratio tell us about HIV and health?, *PLoS Pathog.*, 2017, **13**(11), 1–7, DOI: 10.1371/journal.ppat.1006624.

60 A. Amadori, *et al.*, Genetic control of the CD4/CD8 T-cell ratio in humans, *Nat. Med.*, 1995, **1**(12), 1279–1283, DOI: 10.1038/nm1295-1279.

61 A. Wikby, I. A. Månsson, B. Johansson, J. Strindhall and S. E. Nilsson, The immune risk profile is associated with age and gender: Findings from three Swedish population studies of individuals 20-100 years of age, *Biogerontology*, 2008, **9**(5), 299–308, DOI: 10.1007/s10522-008-9138-6.

62 M. De Zuani, *et al.*, High CD4-to-CD8 ratio identifies an at-risk population susceptible to lethal COVID-19, *Scand. J. Immunol.*, 2022, **95**(3), 1–11, DOI: 10.1111/sji.13125.

63 K. Swiech, K. C. Ribeiro Malmegrim, and V. Picanco-Castro, *Chimeric Antigen Receptor T Cells : Development and Production*. 2020.

64 P. Vormittag, R. Gunn, S. Ghorashian and F. S. Veraitch, A guide to manufacturing CAR T cell therapies, *Curr. Opin. Biotechnol.*, 2018, **53**, 164–181, DOI: 10.1016/j.copbio.2018.01.025.

65 Q. Feng, Z. Liu, X. Yu, T. Huang, J. Chen, J. Wang, J. Wilhelm, S. Li, J. Song, W. Li, Z. Sun, B. Sumer, B. Li, Y. Fu and J. Gao, Lactate increases stemness of CD8 + T cells to augment anti-tumor immunity, *Nat. Commun.*, 2022, **13**(1), 4981, DOI: 10.1038/s41467-022-32521-8.

66 W. J. Quinn, J. Jiao, T. TeSlaa, J. Stadanlick, Z. Wang, L. Wang, T. Akimova, A. Angelin, P. M. Schäfer, M. D. Cully, C. Perry, P. K. Kopinski, L. Guo, I. Blair, L. R. Ghanem, M. S. Leibowitz, W. W. Hancock,

E. K. Moon, M. H. Levine, E. B. Eruslanov, D. C. Wallace, J. A. Baur and U. H. Beier, Lactate Limits T Cell Proliferation via the NAD(H) Redox State, *Cell Rep.*, 2020, **33**(11), 108500, DOI: **10.1016/j.celrep.2020.108500**.

67 E. A. Melkonian and M. P. Schury, *Biochemistry, Anaerobic Glycolysis*, Treasure Island (FL), 2024.

68 E. L. Pearce and E. J. Pearce, Metabolic pathways in immune cell activation and quiescence, *Immunity*, 2013, **38**(4), 633–643, DOI: **10.1016/j.immuni.2013.04.005**.

69 J. T. Grist, *et al.*, Extracellular Lactate: A Novel Measure of T Cell Proliferation, *J. Immunol.*, 2018, **200**(3), 1220–1226, DOI: **10.4049/jimmunol.1700886**.

70 H. L. Caslin, D. Abebayehu, J. A. Pinette and J. J. Ryan, Lactate Is a Metabolic Mediator That Shapes Immune Cell Fate and Function, *Front. Physiol.*, 2021, **12**, 688485, DOI: **10.3389/fphys.2021.688485**.

71 S. F. Ziegler, F. Ramsdell and M. R. Alderson, The activation antigen CD69, *Stem Cell.*, 1994, **12**(5), 456–465, DOI: **10.1002/stem.5530120502**.

72 K. L. Summers, J. L. O'Donnell and D. N. J. Hart, Co-expression of the CD45RA and CD45RO antigens on T lymphocytes in chronic arthritis, *Clin. Exp. Immunol.*, 1994, **97**(1), 39–44, DOI: **10.1111/j.1365-2249.1994.tb06576.x**.

73 A. Rodriguez and J. M. Anderson, Evaluation of clinical biomaterial surface effects on T lymphocyte activation, *J. Biomed. Mater. Res., Part A*, 2010, **92**(1), 214–220, DOI: **10.1002/jbm.a.32362**.

74 R. Craston, M. Koh, A. Mc Dermott, N. Ray, H. G. Prentice and M. W. Lowdell, Temporal dynamics of CD69 expression on lymphoid cells, *J. Immunol. Methods*, 1997, **209**(1), 37–45, DOI: **10.1016/S0022-1759(97)00143-9**.

75 H. K. W. Law, W. Tu, E. Liu and Y. L. Lau, Insulin-like growth factor I promotes cord blood T cell maturation through monocytes and inhibits their apoptosis in part through interleukin-6, *BMC Immunol.*, 2008, **9**, 1–13, DOI: **10.1186/1471-2172-9-74**.

76 L. Pinto, M. J. Covas and R. M. Victorino, Loss of CD45RA and gain of CD45RO after in vitro activation of lymphocytes from HIV-infected patients, *Immunology*, 1991, **73**(2), 147–150, [Online]. Available: **http://www.pubmedcentral.nih.gov/articlerender.fcgi?artid=1384457&tool=pmcentrez&rendertype=abstract**.

77 O. Nájera, *et al.*, CD45RA and CD45RO isoforms in infected malnourished and infected well-nourished children, *Clin. Exp. Immunol.*, 2001, **126**(3), 461–465, DOI: **10.1046/j.1365-2249.2001.01694.x**.

78 M. Niebuhr, *et al.*, Analysis of T cell repertoires of CD45RO CD4 T cells in cohorts of patients with bullous pemphigoid: A pilot study, *Front. Immunol.*, 2022, **13**, 1–13, DOI: **10.3389/fimmu.2022.1006941**.

79 P. H. Mehta, S. Fiorenza, R. M. Koldej, A. Jaworowski, D. S. Ritchie and K. M. Quinn, T Cell Fitness and Autologous CAR T Cell Therapy in Haematologic Malignancy, *Front. Immunol.*, 2021, **12**, 1–15, DOI: **10.3389/fimmu.2021.780442**.

80 L. Gattinoni, D. E. Speiser, M. Lichterfeld and C. Bonini, T memory stem cells in health and disease, *Nat. Med.*, 2017, **23**(1), 18–27, DOI: **10.1038/nm.4241**.

81 I. Raphael, S. Nalawade, T. N. Eagar and T. G. Forsthuber, T cell subsets and their signature cytokines in autoimmune and inflammatory diseases, *Cytokine*, 2015, **74**(1), 5–17, DOI: **10.1016/j.cyto.2014.09.011**.

82 C. Dong, Cytokine Regulation and Function in T Cells, *Annu. Rev. Immunol.*, 2021, **39**, 51–76, DOI: **10.1146/annurev-immunol-061020-053702**.

83 B. Liu, W. Chen, B. D. Evavold and C. Zhu, Accumulation of dynamic catch bonds between TCR and agonist peptide-MHC triggers T cell signaling, *Cell*, 2014, **157**(2), 357–368, DOI: **10.1016/j.cell.2014.02.053**.